TISSUE ENGINEERING: Part A
Volume 19, Numbers 9 and 10, 2013

DOI: 10.1089/ten.tea.2011.0701

Sequential Application of Steady and Pulsatile Medium Perfusion Enhanced the Formation of Engineered Bone

Cristina Correia, PhD,[1–3] Sarindr Bhumiratana, PhD,[1] Rui A. Sousa, PhD,[2,3] Rui L. Reis, PhD,[2,3] and Gordana Vunjak-Novakovic, PhD[1]

In native bone, cells experience fluctuating shear forces that are induced by pulsatile interstitial flow associated with habitual loading. We hypothesized that the formation of engineered bone can be augmented by replicating such physiologic stimuli to osteogenic cells cultured in porous scaffolds using bioreactors with medium perfusion. To test this hypothesis, we investigated the effect of fluid flow regime on *in vitro* bone-like tissue development by human adipose stem cells (hASC) cultivated on porous three-dimensional silk fibroin scaffolds. To this end, we varied the sequential relative durations of steady flow (SF) and pulsatile flow (PF) of culture medium applied over a period of 5 weeks, and evaluated their effect on early stages of bone formation. Porous silk fibroin scaffolds (400–600 μm pore size) were seeded with hASC (30×10^6 cells/mL) and cultured in osteogenic medium under four distinct fluid flow regimes: (1) PF for 5 weeks; (2) SF for 1 week, PF for 4 weeks; (3) SF for 2 weeks, PF for 3 weeks; (4) SF for 5 weeks. The PF was applied in 12 h intervals, with the interstitial velocity fluctuating between 400 and 1200 μm/s at a 0.5 Hz frequency for 2 h, followed by 10 h of SF. In all groups, SF was applied at 400 μm/s. The best osteogenic outcomes were achieved for the sequence of 2 weeks of SF and 3 weeks of PF, as evidenced by gene expression (including the PGE2 mechanotransduction marker), construct compositions, histomorphologies, and biomechanical properties. We thus propose that osteogenesis in hASC and the subsequent early stage bone development involve a mechanism, which detects and responds to the level and duration of hydrodynamic shear forces.

Introduction

The development and function of native bone largely depends on the balance between the endocrine drive towards bone resorption (by a number of biochemical and hormonal factors), and the mechanically-induced drive towards bone formation.[1,2] A healthy balance between these two opposing factors is based on the biological mechanotransduction mechanisms, which may include streaming and piezoelectric potentials, damage to the extracellular matrix, and direct transduction of matrix strain.[3] The most widely accepted stimulator of bone cells *in vitro* has been fluid flow, similar to that generated by loading-induced pressure gradients that stimulate the flow of interstitial fluid through the lacuno-canalicular porosities.[4–6]

Beneficial effects of flow on osteogenic differentiation and bone cells have been observed already in cell monolayers.[7–9] The promising results of cell monolayer studies inspired the application of fluid flow in bone tissue engineering (TE), with the aim to improve quality of tissue, and/or reduce the time of culture. Both primary osteoblasts and bone marrow mesenchymal stem cells, known to have strong osteogenic properties, improved bone tissue formation when cultured under flow conditions as compared to static culture.[10–14] Human adipose tissue derived stem cells (hASC) were also used to engineer bone with the application of interstitial fluid flow.[15,16]

In recent years, hASC have been generating a great deal of interest in the fields of TE and regenerative medicine. Multiple independent studies have proven their ability to selectively differentiate into chondrogenic, osteogenic, and adipose cell lineages,[17] and that this differentiation potential was not different from what was observed from the bone marrow-derived mesenchymal stem cells (BM-MSC).[16] ASCs offer several advantages that make them a promising cell source for bone TE: adipose tissue is abundant, rapidly accessible, with possibility of repeated accessibility; the isolation process is simple, enzyme-based, and results in high yield of cells per unit tissue volume (TV),[16,17] and—with the increased incidence of obesity—high volumes of adipose

[1]Laboratory for Stem Cells and Tissue Engineering, Department of Biomedical Engineering, Columbia University, New York, New York.
[2]3B's Research Group—Biomaterials, Biodegradables and Biomimetics, University of Minho, Headquarters of the European Institute of Excellence on Tissue Engineering and Regenerative Medicine, Guimarães, Portugal.
[3]ICVS/3B's—PT Government Associate Laboratory, Guimarães, Portugal.

tissue resulting from liposuction procedures may be potentially used for cell based therapies.[18]

While fluid flow has been successfully used as stimulator for *in vitro* bone tissue development, the long-term differential effects of steady versus fluctuating shear stress on osteogenesis and bone-like tissue formation were not investigated. Physiologic shear stresses acting on the cells are generated by flow of interstitial fluid, and are intrinsically dynamic. According to Bacabac *et al.*, the frequency spectra of the forces acting on the human hip reach 1–3 Hz for walking and 8–9 Hz for running cycles.[19] Regarding the effect of shear stress on cell monolayers, Jacobs *et al.*, demonstrated that pulsing flow was a much higher stimulator than oscillating flow.[3] Jaasma and O'Brein, using a TE approach, proved that intermittent flow proved advantageous for mechanically stimulating osteoblasts.[20] Several studies have utilized primary osteoblasts and osteocytes,[21,22] and cell lines[7,8,20] to demonstrate advantage of dynamic over steady shear stress. Taken together, these studies suggest that differentiated bone cells are capable of sensing environmental shear stresses.[23,24]

In this context, it is of great interest to investigate the temporal responsiveness of stem cells differentiation to such environments, over periods of time that are relevant to the development of bone. We hypothesized that the formation of bone-like tissue by hASC can be augmented by a sequence of steady and fluctuating shear stress that mediate osteogenic differentiation and subsequent assembly of bone matrix. To test this hypothesis, we investigated the application of steady and pulsatile perfusion combinations, with different relative durations of both regimes, and evaluated the effect of these regimes on osteogenic differentiation of hASC cultivated in silk fibroin scaffolds. Silk fibroin is a potent alternative to other biodegradable biopolymers for bone TE, due to its tunable architecture, degradability and mechanical properties.[12,25–27] Porous sponges produced by silk fibroin have proven adequate structure and biomechanics to support hASC osteogenic differentiation, and bone-like tissue formation demonstrated by bone protein production, calcium deposition, and total bone volume (BV).[27,28] Additionally, this silk fibroin scaffold has supported concomitant angiogenic and osteogenic differentiation of hASC, towards the development of functional vascularized bone grafts.[28]

Materials and Methods

Preparation of silk fibroin scaffolds

All chemicals were purchased from Sigma-Aldrich unless otherwise stated. Hexafluoro-2-propanol (HFIP)-derived silk fibroin scaffolds were prepared as previously described.[29] Silk fibroin from silkworm (*Bombix mori*) cocoons was extracted with 0.02 M sodium carbonate (Na_2CO_3) solution, rinsed in distilled water, dissolved in a 9.3 M lithium bromide (LiBr) solution, and dialyzed for 48 h against distilled water in benzoylated dialysis tubing (Sigma D7884). Dissolved silk fibroin was centrifuged for 20 min at 9000 rpm (4°C). The resulting solution was determined by weighing the remaining solid after drying, yielding a 6-wt% aqueous silk fibroin solution. Silk fibroin aqueous solution was lyophilized and further dissolved with HFIP, resulting in a 16-wt% HFIP-derived silk fibroin solution. Four grams of granular NaCl, particle size 500–600 μm, were added to 2 mL of silk fibroin in HFIP. The containers were covered overnight to reduce evaporation of HFIP and to provide sufficient time for homogeneous distribution of the solution. Subsequently the solvent was evaporated at room temperature for 3 days. The matrices were then treated in 90% (v/v) methanol for 30 min, to induce the formation of β-sheet structure, followed by immersion in water for 2 days to remove NaCl. The porous silk scaffolds were then freeze-dried, and cored into cylinder of 4 mm in diameter and 4 mm thick.

Isolation, characterization, and expansion of hASC

hASC were isolated according to previously established methods[30] from liposuction aspirates of subcutaneous adipose tissue, that were obtained from the Pennington Biomedical Research Center under a protocol approved by the Institutional Research Board. hASC were expanded to the fourth passage (P4) in high-glucose Dulbecco's modified Eagle's medium (DMEM) (Gibco 11965) supplemented with 10% fetal bovine serum (FBS) (Gibco 26140), penicillin–streptomycin (1%) (Gibco 15140), and 1 ng/mL basic fibroblast growth factor (Peprotech 100-18B). p0 cells were examined for surface marker expression using flow cytometry. The presence of specific antigens, such as CD29, CD105, CD45, CD34, CD44, CD73, and CD90 were analyzed, as previously published.[30,31] hASC were tested for their differentiation capacity into the osteogenic, chondrogenic, and adipogenic lineages.

Cell seeding of silk scaffolds

Scaffolds were sterilized in 70% (v/v) ethanol overnight, washed in a phosphate-buffered saline (PBS), and incubated in culture media before seeding. Expanded hASC at passage 4 were suspended at 30×10^6 cells/mL. A 40 μL aliquot of cell suspension was pipetted to the top of blot-dried scaffods, pipetted up and down to ensure even distribution of cells. After 15 min in the incubator, scaffolds were rotated 180°, and 10 μL of cell-free medium was added to prevent these to dry. This process was repeated four times, to allow uniform cell distribution, after which, osteogenic media (low glucose DMEM, 10% FBS, 1% penicillin–streptomycin, 10 mM sodium-b-glycerophosphate, 10 mM HEPES, 100 nM dexamethasone, and 50 μg/mL ascorbic acid-2-phosphate)[15,32] was added. Scaffolds were then cultured in static conditions (well-plate) for 3 days to allow cell attachment.

Bioreactor cultivation of tissue constructs

The experimental design is schematically shown in Figure 1. Cell-seeded scaffolds were transferred into the perfusion bioreactors using a setup already described in previous works (Fig. 1A).[10–12,15] The perfusion bioreactor system has the dimensions of a 10-cm glass Petri dish, and the glass cover of this dish serves as the removable bioreactor cover. It allows culturing multiple scaffolds (4–10 mm in diameter and up to 4 mm high) and imaging capabilities. Scaffolds are placed into six wells arranged in a radial pattern, press fit in place into a layer of polydimethylsiloxane. Each bioreactor enabled simultaneous cultivation and uniform perfusion of the six scaffolds. Culture medium enters the bioreactor through a central port from where it flows to the center of the bioreactor and is evenly distributed into six channels leading

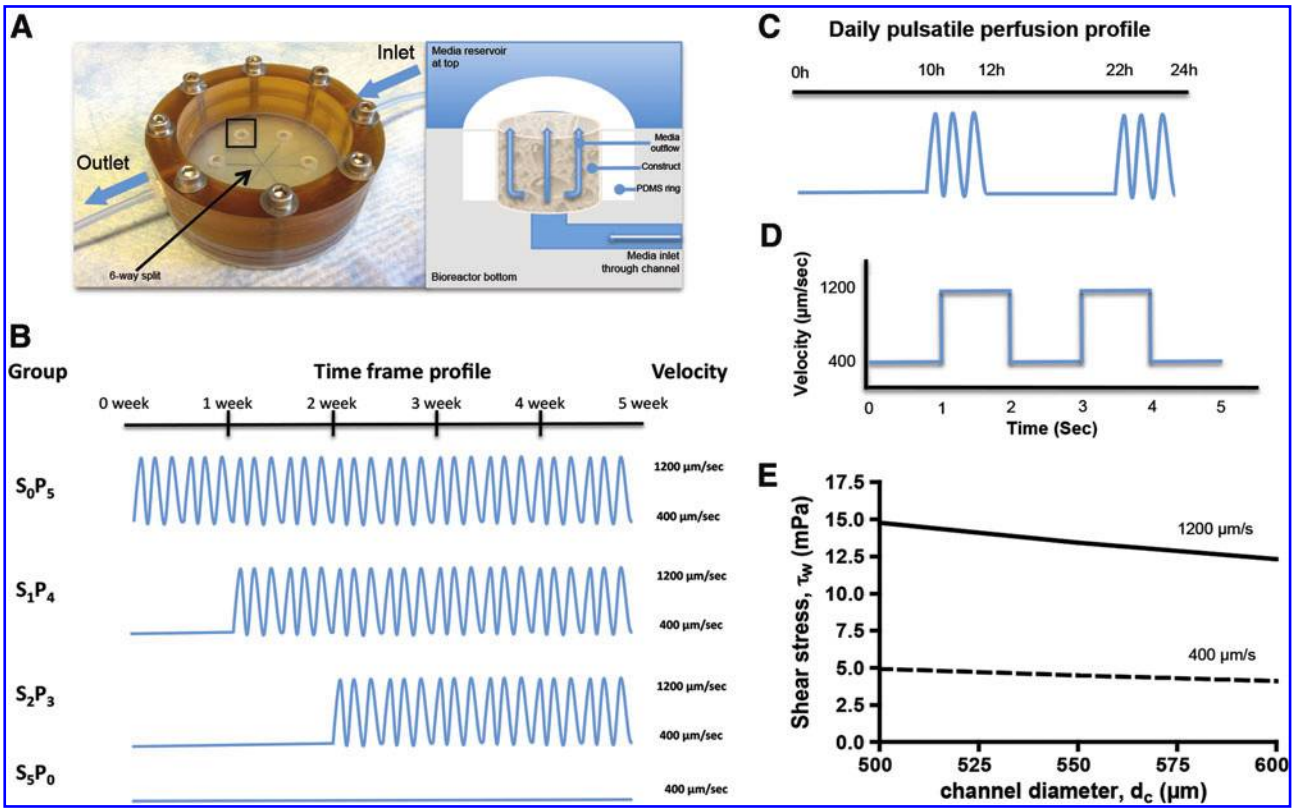

FIG. 1. Experimental design. Bone tissue constructs were engineered by cultivation of human adipose tissue-derived stem cells in porous silk fibroin scaffolds with medium perfusion through the developing tissue. **(A)** Picture and schematic of perfusion bioreactor. Left panel: the system allows simultaneous culturing of six constructs. Arrows indicate directions of medium flow, which is equally distributed through the six channels. The region highlighted by a rectangle is detailed in right panel. Right panel: Medium flows from bottom channel to top medium reservoir throughout the construct, as indicated by arrows. **(B)** The following perfusion regimes were applied: S_0P_5 (pulsatile perfusion for 5 weeks); S_1P_4 (steady perfusion for 1 week, pulsatile perfusion for 4 weeks); S_2P_3 (steady perfusion for 2 weeks, pulsatile perfusion for 3 weeks); S_5P_0 (steady perfusion for 5 weeks). **(C)** Daily pulsatile perfusion profile: 2 h of pulsatile flow followed by 10 h of steady flow. **(D)** Curve of pulsatile flow at 0.5 Hz. **(E)** Estimated maximum and minimum shear stress generated in scaffold pores (500–600 µm diameter), at the fluid flow velocities of 400 and 1200 µm/s. Color images available online at www.liebertpub.com/tea

to the scaffolds. A multichannel peristaltic pump (Ismatec) is used to maintain recirculating flow. The flow rate was determined by the cross-sectional area of the tube as the length of the column of fluid being pumped and the rate of pumping remained constant among groups. Four experimental groups were established by varying the relative durations of steady flow (SF) and pulsatile flow (PF) as follows: S_0P_5: PF for 5 weeks; S_1P_4: SF for 1 week, PF for 4 weeks; S_2P_3: SF for 2 weeks, PF for 3 weeks; S_5P_0: SF for 5 weeks (Fig. 1B). Pulsatile fluid flow regime was composed of flow velocities varying between 400 µm/s (1.64 mL/min) and 1200 µm/s (4.92 mL/min), at 0.5 Hz frequency for 2 h, followed by 10 h of SF (Fig. 1C, D). In all groups, SF was applied at a flow velocity of 400 µm/s. The maximum and minimum shear stress generated in scaffold pores, ranging from 500 to 600 µm, was estimated of about 4–5 mPa at 400 µm/s and 12.5–15 mPa at 1200 µm/s (Fig. 1E).

Live/dead assay

Live/dead Viability/Citotoxicity kit (Molecular Probes) was used to evaluate cell viability. Live cells (indicated by Calcein acetoxymethylester [AM]) and dead cells (indicated by Ethidium homodimer-1 [EthD-1]) were imaged through a confocal microscope (Leica). All scaffolds were cut in half, and the entire scaffold area was imaged from both bulk to edge, and edge to bulk. Optical sections were made parallel to the external surface in 10 µm intervals up to 160 µm deep, and presented as vertical projections. Several images were obtained to ensure even distribution and viability of cells, and the most representative, obtained from bulk to edge, was selected.

Biochemical characterization

Constructs were harvested at timed intervals, washed in the PBS, dry blotted, cut in half, and weighed. For DNA assay, one half was added to 1 mL of digestion buffer (10 mM Tris, 1 mM ethylenediaminetetraacetic acid, 0.1% Triton X-100, 0.1 mg/mL proteinase K) and incubated overnight at 56°C for digestion. After centrifugation at 3000 *g* for 10 min, the supernatants were removed, diluted, pipetted in duplicate into a 96-well plate, and a 1:1 ratio of Picogreen solution (Quant-iT™ PicoGreen® dsDNA Kit; Invitrogen) was added. Sample fluorescence was measured with fluorescent plate reader at excitation ~480 nm, and emission ~520 nm.

Lambda DNA was used to prepare the standard curve. For calcium quantification, one half of constructs were incubated in 1 mL trichloroacetic acid (TCA) 5% (TCA 5% v/v) and calcium was extracted by disintegrating the construct using steel balls and MinibeadBeater™ (Biospec). The supernatant were transferred in duplicate into 96-well plate and calcium binding reagent was added at 1:10 ratio (StanbioTotal Calcium Liquicolor®; Stanbio Laboratory). Sample optical density was measured using a microplate reader set to 575 nm. Calcium standard was used to prepare the standard curve.

Immunohistochemistry

Samples were fixed in 10% formalin for 1 day, embedded in paraffin, sectioned to 5 μm and mounted on glass slides. Sections were deparaffinized with CitriSolv and rehydrated in a graded series of ethanol washes. For immunohistochemistry, sections were blocked with normal horse serum (NHS), stained sequentially with primary antibody (rabbit antihuman osteopontin [OPN] polyclonal antibody; Chemicon ab1870, rabbit antibone sialoprotein [BSP] polyclonal antibody; Millipore ab1854, NHS for negative control), secondary antibody (Vectastain Universal Elite ABC Kit; PK-6200 Vector Laboratories), and developed with biotin-avidin system (DAB substrate kit SK-4100; Vector Laboratories). Imaging was performed using a Transmitted and Reflected Light Microscope (Axioimager Z1M; Zeiss), and semiquantitative evaluation of protein deposition was obtained by measuring stain density of immunohistochemical images using ImageJ software (1.44o; NIH).

Microcomputed tomography analysis

Microcomputed tomography (μCT) analysis was performed using an established protocol.[33] Samples were aligned in a 2 mL screw cap centrifuge tube that was clamped in the specimen holder of a vivaCT40 system (SCANCO Medical AG). Four millimeter length of each scaffold was scanned at 21 μm isotropic resolution. A global thresholding technique, which only detects mineralized tissue, was applied to obtain the BV of samples.

Real-time reverse-transcription-polymerase chain reaction

For RNA extraction, one half of constructs were added to 800 μL of Trizol (Invitrogen 15596-026) and disintegrated by using steel balls and MinibeadBeater (Biospec). Suspensions were centrifuged at 12,000 *g* for 10 min at 4°C to remove tissue debris and extracted with chloroform (Sigma C2432). Colorless aqueous phase, containing RNA was removed and mixed with equal volume of isopropanol (Sigma I9516). Suspensions were again centrifuged at 12,000 *g* for 8 min at 4°C, supernatant discarded, and RNA pellet washed with 75% ethanol. Samples were centrifuged at 7500 *g* for 5 min at 4°C, supernatant removed, pellet air-dried, and dissolved with diethylpyrocarbonate-water (Applied Biosystems AM 9920). RNA was quantified using Nanodrop® ND-1000. Approximately 1 μg of RNA was reversely transcribed with random hexameres using High Capacity cDNA Reverse Transcription Kit (Applied Biosystems 4368814).

OPN, BSP, prostaglandin E2 synthase (PGE_2S), and the housekeeping gene glyceraldehyde-3-phosphate dehydrogenase (GAPDH) expression were quantified using a 7500 Fast Real-Time PCR System (Applied Biosystems). Gene expression assay ID, probe, and amplicon size and are described on Table 1. All TaqMan® Gene Expression Assays were purchased from Applied Biosystems. The expression data were normalized to GAPDH and presented as average values for each group.

Mechanical testing

The equilibrium Young's modulus of constructs was determined before and after culturing, under unconfined compression in wet conditions using a modification of an established protocol.[34] An initial tare load of 0.2 N was applied to each sample. Specimens were compressed at a strain rate of 1%/s up to 10% strain and subsequently maintained at this strain for 1800 s. The Young's modulus was obtained from the equilibrium stress measured at 10% strain.

Statistical analysis

Data are presented as average ± standard deviation ($n = 3$). Statistical significance was determined using analysis of variance followed by Tukey's honestly significant difference test using Prism software (Prism 4.0c; GraphPad Software, Inc.).

Results

Cell proliferation and viability

After 5 weeks of dynamic bioreactor cultivation, the amounts of DNA increased over initial values in all groups, reaching levels that were slightly but not significantly different among the experimental groups (Fig. 2, top). Live/dead viability assay allowed the observation, by confocal microscopy, of green viable cells, which enzymatically converted nonfluorescent cell-permeant calcein AM into the intensely fluorescent calcein, and dead cells identified by bright red fluorescense of EthD-1 bound to nucleic acids of cells with damaged membranes (Fig. 2, bottom). Viable cells throughout scaffold surfaces were observed in all experimental groups.

Bone tissue development

Bone extracellular matrix markers, such as OPN and BSP were detected by both gene expression (GE) and protein deposition constructs harvested after 5 weeks of culture. OPN GE profiles corroborates measured bone protein deposition (Fig. 3, top), with highest OPN GE quantified for the S_2P_3 group and lowest OPN GE for S_5P_0 group. These values

Table 1. Gene Expression Assays Used for Quantitative Reverse-Transcription-Polymerase Chain Reaction

Gene	*GEA ID*	*Probe*	*Amplicon (bp)*
Osteopontin	Hs00167093_m1	FAM	35
Bone sialoprotein	Hs00173720_m1	FAM	95
Prostaglandin E_2 synthase	Hs00228159_m1	FAM	36
GAPDH	Hs99999905_m1	FAM	122

GEA, gene expression assay; bp, base pairs; GAPDH, glyceraldehyde 3-phosphate dehydrogenase.

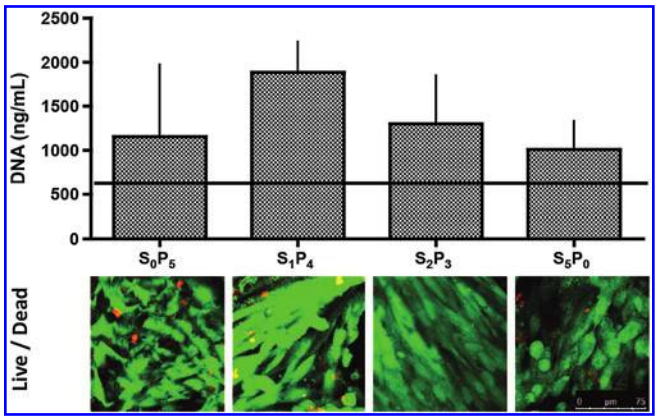

FIG. 2. Cell proliferation and viability. Top: Amount of DNA in tissue constructs at the end of the 5-week culture period; the horizontal line indicates day 1 value ($n=3$). Bottom: Live/dead imaging of constructs after 5 weeks of culture. Scale bar = 75 μm. Color images available online at www.liebertpub.com/tea

were significantly different ($p<0.05$). OPN gene GE progressively increased with the increase of osteogenic predifferentiation period before application of pulsatile regimen: OPN GE_{S0P5} < OPN GE_{S1P4} < OPN GE_{S2P3}. BSP GE was not different among the groups studied. GE of PGE_2S was also quantified, since prostaglandin E2 (PGE_2) release is stimulated by shear stress in a dose-dependent manner[6] (Fig. 3, bottom). This paracrine factor was also highly expressed by hASC cultured in S_2P_3 pulsatile regimen, and significantly different ($p<0.05$) from the S_5P_0 group that was not subjected to pulsatile fluid flow during culture. As observed for OPN, PGE_2S GE progressively increased with the increase of osteogenic predifferentiation period before application of a pulsatile regimen: PGE_2S GE_{S0P5} < PGE_2S GE_{S1P4} < PGE_2S GE_{S2P3}.

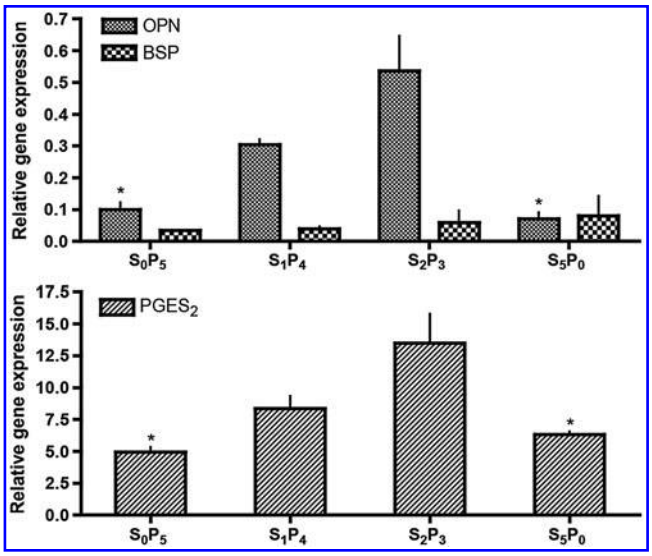

FIG. 3. Gene expression after 5 weeks of culture. Top: osteopontin (OPN) and bone sialoprotein (BSP) gene expression normalized to glyceraldehyde 3-phosphate dehydrogenase (GAPDH) ($n=3$) *$p<0.05$ relatively to S_2P_3. Bottom: Prostaglandin E2 synthase (PGE_2S) gene expression normalized to GAPDH ($n=3$) *$p<0.05$ relative to S_2P_3.

Bone protein deposition was further assessed through immunolocalization in cross-sections of constructs (Figs. 4 and 5). OPN deposition was clearly enhanced in all groups subjected to pulsatile fluid flow (PF) in comparison to the experimental group cultured under steady fluid flow (SF). The same trend was observed for the deposition of BSP and collagen type I (Col I). No significant differences were detected for osteocalcin (OCN) deposition. This trend was confirmed by semiquantitative evaluation of protein deposition obtained by measuring stain density of immunohistochemical images through ImageJ software (Fig. 6). Among the three groups subjected to PF, we observed significant increase of bone protein deposition in S_2P_3 group (OPN $p<0.01$, BSP $p<0.05$ and Col I $p<0.01$, relatively to S_5P_0), where cell-seeded scaffolds were cultured under steady fluid flow (SF) for 2 weeks, before the application of pulsatile fluid flow (PF) during 3 weeks.

Mineralization was assessed through calcium quantification, and BV normalized by TV (BV/TV) (Fig. 7). The highest amount of calcium was obtained with the S_2P_3 culturing regimen, again significantly different ($p<0.05$) from S_5P_0 group where the lowest amount was quantified (Fig. 7, top). BV/TV ratio corroborates calcium data and μCT reconstruction images, where S_2P_3 present the highest ratio and S_5P_0 the lowest (Fig. 7, middle). Constructs cultured under any regimen of PF demonstrated increased deposition and more uniform distribution of mineral throughout the scaffold as compared to constructs cultured exclusively under SF, as evidenced by μCT reconstruction (Fig. 7, bottom). Among the three pulsatile regimens, S_2P_3 was the one that stimulated best mineralization of hASC, as shown by compact mineral deposition detected by μCT.

Mechanical properties of cultured constructs are presented in Figure 8. After culture, scaffolds became stiffer, although no statistical difference was detected among groups. In average, equilibrium modulus increased 1.8× by the end of culture.

Discussion

Perfusion bioreactors have been used in TE with the main purpose to improve gas transfer, nutrient supply and waste removal between tri-dimensional constructs and culture medium by reducing diffusional distances.[35,36] Several studies have explored the use of perfusion to improve osteogenic differentiation and bone-like tissue formation with primary osteoblasts, BM-MSC,[11–14] and hASC.[15] Yet, to our knowledge, variations of flow rate during culturing period have not been implemented in perfusion studies, where SF and inherent constant shear stress are commonly used. The effects of steady culturing regimen are intrinsically different from native situation, where shear caused by movement of interstitial fluid is not constant. In the present work, we aimed to more closely mimic physiologic nature by creating a sequence of steady and PFs, and consequently augment bone-like tissue development by hASC osteogenic differentiation, in porous silk scaffolds. We also aimed to understand the importance of osteogenic predifferentiation of hASC in the achievement of this goal. Our aim was accomplished, as all PF regimes improved early stage development of bone

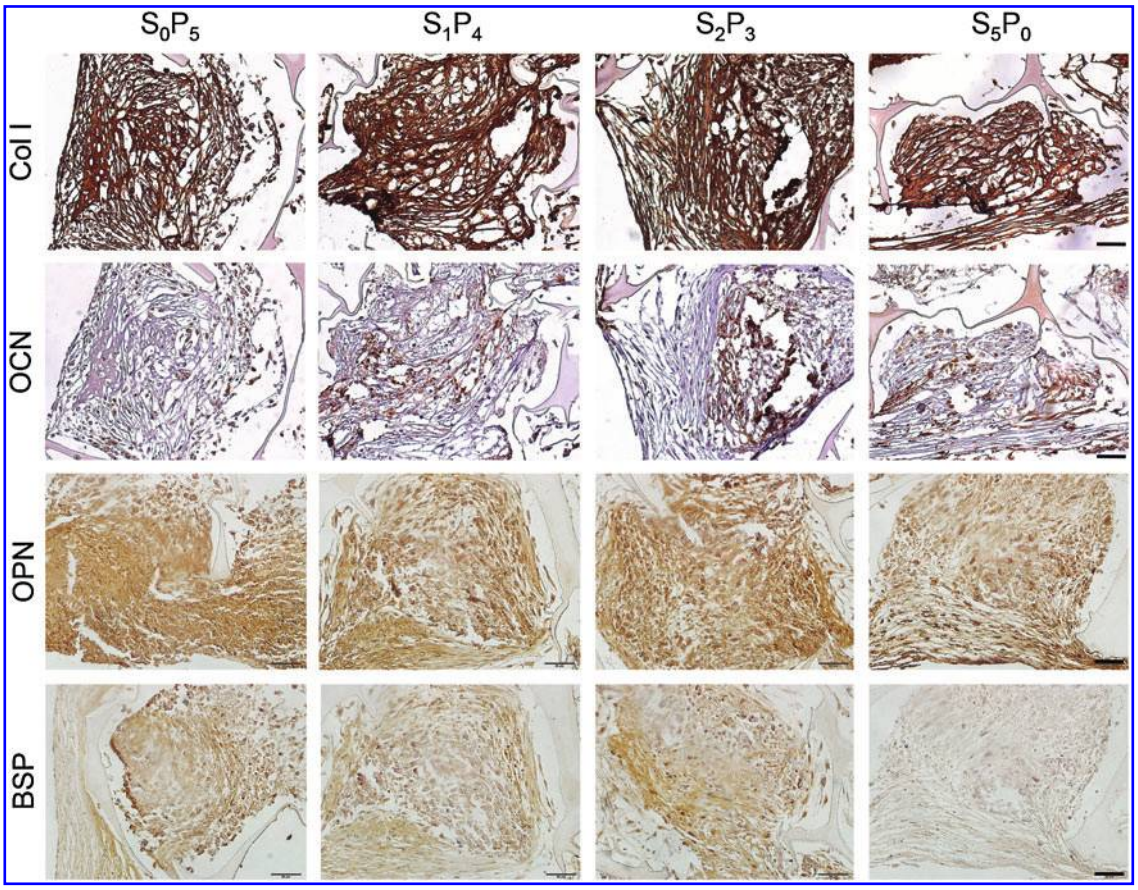

FIG. 4. Immunohistochemical localization of osteogenic proteins. Collagen type I (Col I), osteocalcin (OCN), OPN and BSP were detected after 5 weeks of culture. Scale bar = 50 μm. Color images available online at www.liebertpub.com/tea

tissue over SF, and the best outcomes were obtained for 2 weeks of osteogenic predifferentiation preceding pulsatile regime.

In native bone, cells experience dynamic mechanical shear force[4,37] due to the flow of interstitial fluid resulting from physical movement.[9,38,39] Ideally, bone TE should mimic such physiologic environment in which medium flow is dynamic and, hence, shear stress is variable. Previous studies demonstrated the positive effect of static shear force on osteogenic differentiation and tissue engineered bone formation[10–12,15]; however, the physiologic shear force is not static.[23,39] We hypothesized that osteogenic cells do not only respond to shear force but also to time and dynamic range of shear force application. In this study, we explored the dynamic flow paradigm by applying a sequence of steady and pulsatile fluid flows, SF and PF, respectively, to hASC in silk fibroin scaffolds, in the context of bone TE.

To estimate the hydrodynamic shear stress acting at cells within scaffolds (τ_w), we have modeled the interconnected pore network of scaffolds as a bundle of parallel, cylindrical channels with an average diameter of 550 μm (d_c). In this model, we have considered a sufficient number of channels that assures a porosity of 90%, as in one of our previous studies.[12] According to our estimates, using the equation $\tau_w = (8\,\mu)/d_c$ derived from the Hagen-Poiseuille relation for laminar flow through a conduit (= mean linear flow rate), the calculated shear stress within tissue constructs ranged from 4.48 mPa (0.045 dyn/cm^2) to 13.44 mPa (0.134 dyn/cm^2) at flow velocities of 400 to 1200 μm/s, respectively. According to the theoretical model proposed by Weinbaum *et al.*,[23] the magnitude of the fluid induced shear stresses *in vivo* is in the range of 8–30 dyn/cm^2. In our study, we did not reach these high levels of shear stress associated with the mature bone, but instead attempted to mimic the *in vivo* pulsatile profile for developing bone. To this end, we varied shear stress at a lower level, with a threefold difference between the minimum and maximum shear stress levels (0.045–0.134 dyn/cm^2) (Fig. 1E). Yet, it is expected that fluid dynamics change through the scaffold during extended culturing, given cell proliferation, deposition of extracellular matrix by differentiating cells, as well as some extent of scaffold degradation. Accordingly, when pore diameter (d_c) decreases by filling of the pore space, shear stress sensed by the cells lining along the opening space increase, possibly approaching physiologic values.

In terms of frequency, we have used a regimen (0.5 Hz) that resembles the dynamic force spectra applied to the human hip during slow walking.[19] Based in previous studies of our research group,[10] the optimal range of flow velocities that resulted in the highest matrix deposition were of 400–800 μm/s, while 1200–1800 μm/s flow velocity resulted in low OPN quantification, and elongated cell morphologies. Accordingly, 400 μm/s was applied for the steady and control flows.

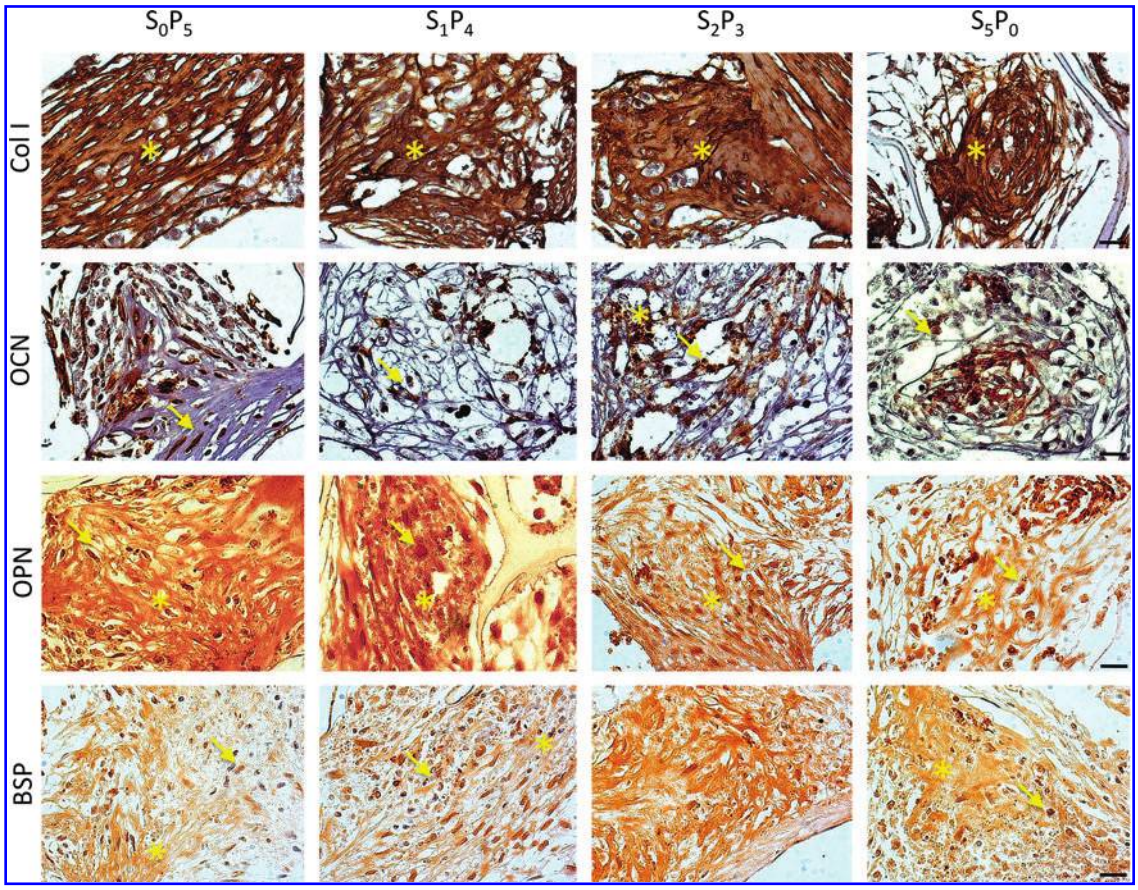

FIG. 5. Immunohistochemical localization of osteogenic proteins. Col I, OCN, OPN and BSP were detected after 5 weeks of culture. *Indicates antibody immunoreactivity at the extracellular level. Arrow indicates immunoreactivity at the intracellular level. Scale bar = 20 μm. Color images available online at www.liebertpub.com/tea

As one of the drawbacks in perfusion culturing is the possibility of cell "wash out" from the scaffold, we assessed cell viability and proliferation and observed viable cells attached throughout the scaffold surface for all studied groups, as well as an increase in cell numbers at the end of culture (Fig. 2). Despite this increase, DNA quantification denotes minimal growth in the 5 weeks of culture. Cell proliferation and differentiation are mutually exclusive events; therefore it is not surprising to observe low levels of cell proliferation once high differentiation stimuli are provided (both biochemical and biomechanical). No significant differences were detected between groups, suggesting that proliferation occurred to a similar extent despite differences in fluid flow regimen.

The constructs subjected to pulsatile fluid flow during 5 weeks demonstrated superior bone-like development in terms of GE (Fig. 3) and protein deposition (Figs. 4 and 5) of osteogenic markers, such as OPN, OCN, Col I, and BSP. Notably, OPN is a mechanosensitive gene, encoding the extracellular bone matrix protein OPN, which has been used to assess bone cell mechanoresponsiveness.[40–42] Significant differences were detected at both GE and protein secretion (detected at both intra and extracellular level).

BSP mRNA expression was also studied to prove bone-like tissue development induced by mechanical signals.[43] While no significant differences were detected regarding GE at this 5-week time-point, significantly higher protein deposition was observed by immunohistochemistry in S_2P_3 group subjected to PF, in comparison to the SF group (Fig. 6, $p < 0.01$). This might be explained by the dynamics of the DNA-mRNA-protein cascade, with differences in mRNA expression (which we have not detected as only the late time points were analyzed) preceding the differences in protein expression (which have been detected, Fig. 6). In particular, one of the functions of the BSP is to act as a nucleus for the initial formation of the apatite crystals. Consistently, we found increased mineral deposition (evidenced by quantitative μCT) in the groups cultured under PF (Fig. 7), suggesting the stimulatory role of PF in deposition of mineralized matrix.

Col I protein deposition was detected at the extracellular level, and staining intensity followed similar trend, occupying significantly higher % area of engineered tissue in S_2P_3 group ($p < 0.01$), relatively to constructs cultured under SF the total 5 weeks of culture (S_5P_0) (Figs. 4–6). OCN was immunolocalized in construct sections mostly at the intracellular level (not yet secreted), and no significant differences were determined among groups. OCN is secreted solely by osteoblasts therefore, it is not surprising that this protein is present in less extent than OPN, BSP and Col I that are secreted by other cell types, such as preosteoblasts, osteocytes, among others.

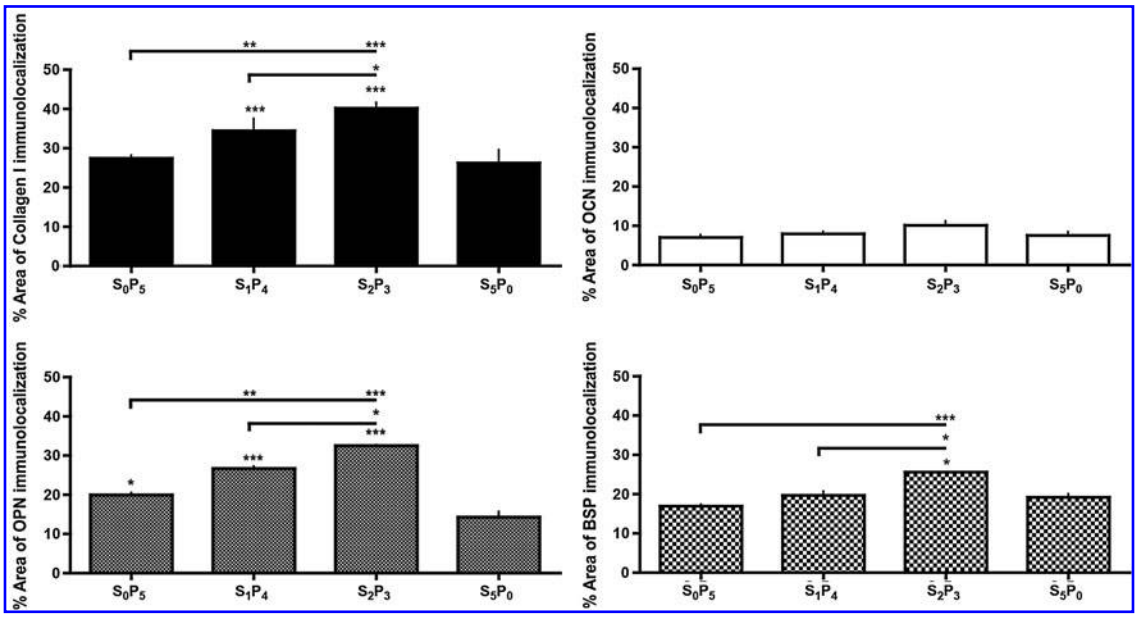

FIG. 6. Semiquantification of osteogenic protein deposition. % area of osteogenic protein deposition was obtained by measuring stain density of immunohistochemical images by ImageJ software. *$p < 0.05$; **$p < 0.01$; ***$p < 0.001$ relatively to S_5P_0.

Increased mRNA expression of PGE_2S (Fig. 4, bottom), corroborate the hASC response to dynamic mechanical stimulation, once PGE_2 is one of the most important markers of mechanically induced bone formation.[7,20,44] Although we have not determined protein expression, it is well described in the literature concurrent detection of PGE_2S mRNA and protein expression.[45–47] In addition to GE and protein deposition, constructs cultured under dynamic shear stress (PF) increased mineralization as compared to constructs cultured under SF (Fig. 7). Mechanical properties of engineered constructs, displayed as equilibrium modulus (Fig. 8), were not statistically different despite differences in mineralization. Increased matrix and mineral deposition were observed in S_2P_3 condition, which led to narrowing of pore diameter within the scaffold structure. The decrease in pore diameter increases shear stress forces applied (according to $\tau_w = (8\,\mu)/d_c$ equation), which may cause higher degradation and or weakening of the silk scaffold structure, and consequently have an effect on its mechanical properties. Increase of mineral content within the structure may compensate mechanical properties, as higher equilibrium modulus was quantified after culture, relatively to beginning of culture. The lack of pulsatile perfusion in condition S_5P_0 resulted in less matrix and mineral deposition, therefore lower shear stress increase, and consequent less scaffold degradation, resulting in similar mechanical properties as those quantified for S_2P_3 group.

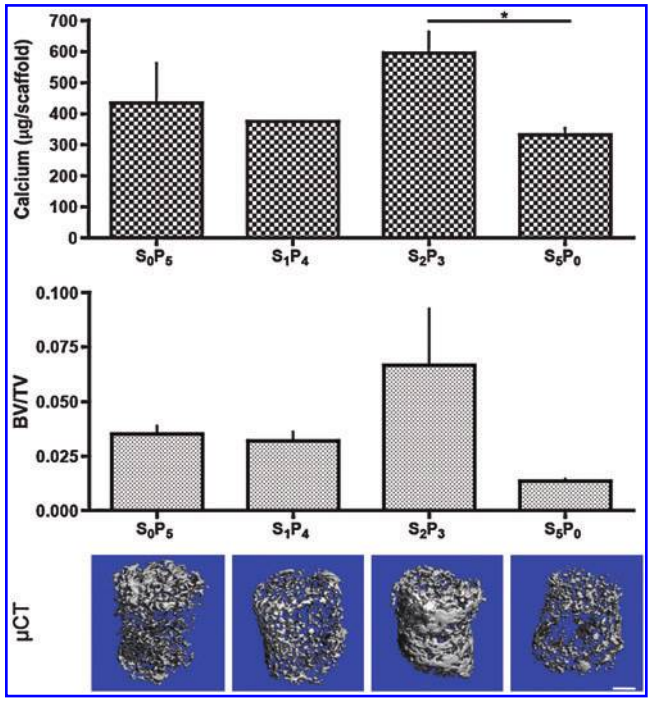

FIG. 7. Deposition of mineralized tissue after 5 weeks of culture. Top: Amount of calcium ($n = 3$), *$p < 0.05$. Middle: Ratio of bone volume (BV) to tissue volume (TV) ($n = 3$). Bottom: Microcomputed tomography reconstruction images of mineralized tissue matrix. Scale bar = 1 mm. Color images available online at www.liebertpub.com/tea

Taken altogether, variation of flow rate, through the application of pulsatile fluid flow seems to augment formation of early stage bone by hASC, relatively to conventional steady fluid flow. Furthermore, we determined the temporal development of the sensing mechanism for the exerted pulsatile forces in hASC osteogenic differentiation. It was previously suggested that communicating osteocytes are the bone cells responsible for sensing small strains in the calcified matrix components of bone, through their osteocytic processes and not through the cell body.[23,24] hASC lack these processes, which may lead to failure to response to mechanical stimuli. Therefore, we assumed that hASC should be first differentiated into the osteogenic lineage to be

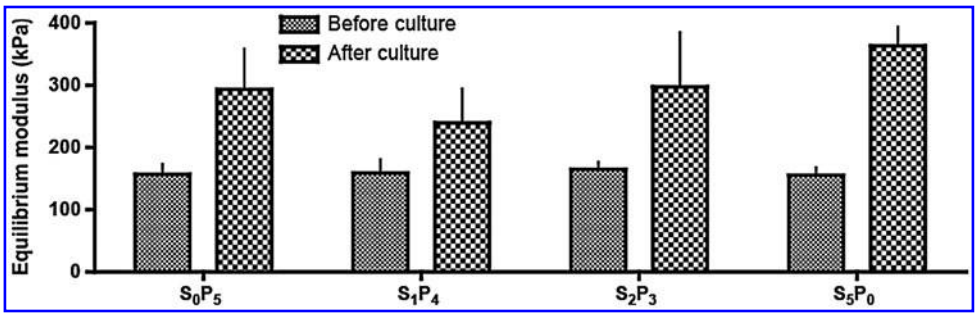

FIG. 8. Biomechanical properties of tissue constructs. Equilibrium modulus measured after 5 weeks of culture is compared to the initial value measured for the scaffold.

capable to sense the pulsatile fluid flow applied by dynamic culture of hASC-seeded silk scaffolds. We have observed osteogenic differentiation of hASC, at same cell density and silk fibroin scaffold, after 2 weeks of static culture,[27] and our group has demonstrated that increased nutrient supply and gas exchange provided by media flow enhance hASC osteogenic differentiation, relatively to static culture.[15] Therefore, hASC-seeded scaffolds were cultured in osteogenic medium, first under steady fluid flow (1 or 2 weeks) and then under pulsatile fluid flow for the remaining culture period (4 or 3 weeks, respectively). The best bone-like tissue development was achieved for hASC predifferentiated for 2 weeks under SF, and only then subjected to the PF regime. Under these conditions, highest increases in bone protein deposition (both OPN and BSP) and the corresponding GE, calcification and BV were detected. Mechanical loading is known to induce expression of PGE_2, an important early stage bone development marker.[44,48] Thus, we looked into GE of PGE_2 synthase to assess if this marker would be differently expressed as response to changes in shear force. Interestingly, we have observed the following progression of PGE_2 synthase and osteogenic differentiation: $S_0P_5 < S_1P_4 < S_2P_3$. These data are in support of our hypothesis that there is a temporal development of the sensing mechanism to the exerted shear stresses upon hASC differentiation, which makes cells to sense differently steady and PF and hydrodynamic shear. Therefore, the mechanisms and key factors involved in mechanotransduction are interesting targets for modulating osteogenic differentiation of hASC under dynamic shear stress, and should be extensively explored.

Conclusion

A bone TE model consisting of hASC cultured in porous silk fibroin scaffolds in a bioreactor with perfusion (interstitial flow) of culture medium was used to investigate the effects of pulsatile versus steady medium flow. Our hypothesis was that a sequence of SF followed by PF will be optimal for supporting bone-like tissue development, first by stimulating osteogenic cell differentiation and, second, by promoting expression of bone tissue matrix. PF ranging from 400 to 1200 μm/s, at 0.5 Hz, associated with fluctuating shear stresses (0.045–0.134 dyn/cm^2) improved early stage bone formation in comparison to SF at 400 μm/s. Furthermore, cell response to pulsatile fluid flow was progressively enhanced with the increase of SF culturing time, being enhanced for 2 weeks of culture. These data are consistent with the notion that osteogenic hASC gradually developed a mechanism to detect and respond to changes in shear stress. Future studies in the broader range of flow rates and flow regimes are necessary to elucidate the individual contributions of the flow regime (pulsatile vs. steady) and the extent and duration of the exposure to shear forces on cell responses in the context of engineered bone formation.

Acknowledgments

We gratefully acknowledge funding support of this work by the NIH (DE161525, AR061988 and EB02520 to G.V.-N.), and the FCT PhD grant (SFRH/BD/42316/2007 to C.C.). The authors thank Dr. Darja Marolt and Supansa Yodmuang for their help with the experiments, Professor David L. Kaplan (Tufts University) for providing silk scaffolds, and Professor Jeffrey M. Gimble (Louisiana State University) for providing adipose stem cells used in this study.

Disclosure Statement

No competing financial interests exist.

References

1. Martin, A.D., and McCulloch, R.G. Bone dynamics: stress, strain and fracture. J Sport Sci **5,** 155, 1987.
2. Jones, H.H., Priest, J.D., Hayes, W.C., Tichenor, C.C., and Nagel, D.A. Humeral hypertrophy in response to exercise. J Bone Joint Surg Am **59,** 204, 1977.
3. Jacobs, C.R., *et al.* Differential effect of steady versus oscillating flow on bone cells. J Biomech **31,** 969, 1998.
4. Burger, E.H., and Klein-Nulend, J. Mechanotransduction in bone—role of the lacuno-canalicular network. FASEB J **13 Suppl,** S101, 1999.
5. Hung, C.T., Pollack, S.R., Reilly, T.M., and Brighton, C.T. Real-time calcium response of cultured bone-cells to fluid-flow. Clin Orthop Relat Res 256, 1995.
6. Reich, K.M., and Frangos, J.A. Effect of flow on prostaglandin-E2 and inositol trisphosphate levels in osteoblasts. Am J Physiol **261,** C428, 1991.
7. Donahue, T.L.H., Haut, T.R., Yellowley, C.E., Donahue, H.J., and Jacobs, C.R. Mechanosensitivity of bone cells to oscillating fluid flow induced shear stress may be modulated by chemotransport. J Biomech **36,** 1363, 2003.
8. Santos, A., Bakker, A.D., Zandieh-Doulabi, B., Semeins, C.M., and Klein-Nulend, J. Pulsating fluid flow modulates gene expression of proteins involved in Wnt signaling pathways in osteocytes. J Orthop Res **27,** 1280, 2009.
9. Knippenberg, M., *et al.* Adipose tissue-derived mesenchymal stem cells acquire bone cell-like responsiveness to

fluid shear stress on osteogenic stimulation. Tissue Eng **11,** 1780, 2005.
10. Grayson, W.L., *et al.* Optimizing the medium perfusion rate in bone tissue engineering bioreactors. Biotechnol Bioeng **108,** 1159, 2011.
11. Grayson, W.L., *et al.* Effects of initial seeding density and fluid perfusion rate on formation of tissue-engineered bone. Tissue Eng Part A **14,** 1809, 2008.
12. Bhumiratana, S., *et al.* Nucleation and growth of mineralized bone matrix on silk-hydroxyapatite composite scaffolds. Biomaterials **32,** 2812, 2011.
13. Gomes, M.E., Holtorf, H.L., Reis, R.L., and Mikos, A.G. Influence of the porosity of starch-based fiber mesh scaffolds on the proliferation and osteogenic differentiation of bone marrow stromal cells cultured in a flow perfusion bioreactor. Tissue Eng **12,** 801, 2006.
14. Martins, A.M., *et al.* Combination of enzymes and flow perfusion conditions improves osteogenic differentiation of bone marrow stromal cells cultured upon starch/poly(epsilon-caprolactone) fiber meshes. J Biomed Mater Res A **94,** 1061, 2010.
15. Frohlich, M., *et al.* Bone grafts engineered from human adipose-derived stem cells in perfusion bioreactor culture. Tissue Eng Part A **16,** 179, 2010.
16. Scherberich, A., Galli, R., Jaquiery, C., Farhadi, J., and Martin, I. Three-dimensional perfusion culture of human adipose tissue-derived endothelial and osteoblastic progenitors generates osteogenic constructs with intrinsic vascularization capacity. Stem cells **25,** 1823, 2007.
17. Gimble, J.M., and Bunnel, B.A. Adipose-Derived Stem Cells: Methods and Protocols, Vol. 702, New York: Springer Science+Business Media, LLC, 2011.
18. Gimble, J.M., Katz, A.J., and Bunnell, B.A. Adipose-derived stem cells for regenerative medicine. Circ Res **100,** 1249, 2007.
19. Bacabac, R.G., *et al.* Nitric oxide production by bone cells is fluid shear stress rate dependent. Biochem Biophys Res Commun **315,** 823, 2004.
20. Jaasma, M.J., and O'Brien, F.J. Mechanical stimulation of osteoblasts using steady and dynamic fluid flow. Tissue Eng Part A **14,** 1213, 2008.
21. Sikavitsas, V.I., Bancroft, G.N., Holtorf, H.L., Jansen, J.A., and Mikos, A.G. Mineralized matrix deposition by marrow stromal osteoblasts in 3D perfusion culture increases with increasing fluid shear forces. Proc Natl Acad Sci U S A **100,** 14683, 2003.
22. Bancroft, G.N., *et al.* Fluid flow increases mineralized matrix deposition in 3D perfusion culture of marrow stromal osteoblasts in a dose-dependent manner. Proc Natl Acad Sci U S A **99,** 12600, 2002.
23. Weinbaum, S., Cowin, S.C., and Zeng, Y. A Model for the excitation of osteocytes by mechanical loading-induced bone fluid shear stresses. J Biomech **27,** 339, 1994.
24. Anderson, E.J., Kaliyamoorthy, S., Alexander, J.I.D., and Tate, M.L.K. Nano-microscale models of periosteocytic flow show differences in stresses imparted to cell body and processes. Ann Biomed Eng **33,** 52, 2005.
25. Meinel, L., *et al.* Engineering bone-like tissue *in vitro* using human bone marrow stem cells and silk scaffolds. J Biomed Mater Res Part A **71A,** 25, 2004.
26. Wang, Y., *et al. In vivo* degradation of three-dimensional silk fibroin scaffolds. Biomaterials **29,** 3415, 2008.
27. Correia, C., *et al.* Development of silk-based scaffolds for tissue engineering of bone from human adipose-derived stem cells. Acta Biomater **8,** 2483, 2012.
28. Correia, C., *et al.* Human adipose derived cells can serve as a single cell source for the *in vitro* cultivation of vascularized bone grafts. J Tissue Eng Regen Med 2012. DOI: 10.1002/term.1564.
29. Kim, U.J., Park, J., Kim, H.J., Wada, M., and Kaplan, D.L. Three-dimensional aqueous-derived biomaterial scaffolds from silk fibroin. Biomaterials **26,** 2775, 2005.
30. McIntosh, K., *et al.* The immunogenicity of human adipose-derived cells: temporal changes *in vitro*. Stem cells **24,** 1246, 2006.
31. Mitchell, J.B., *et al.* Immunophenotype of human adipose-derived cells: temporal changes in stromal-associated and stem cell-associated markers. Stem cells **24,** 376, 2006.
32. Zuk, P.A., *et al.* Multilineage cells from human adipose tissue: implications for cell-based therapies. Tissue Eng **7,** 211, 2001.
33. Liu, X.W.S., Sajda, P., Saha, P.K., Wehrli, F.W., and Guo, X.E. Quantification of the roles of trabecular microarchitecture and trabecular type in determining the elastic modulus of human trabecular bone. J Bone Miner Res **21,** 1608, 2006.
34. Mauck, R.L., *et al.* Functional tissue engineering of articular cartilage through dynamic loading of chondrocyte-seeded agarose gels. J Biomech Eng **122,** 252, 2000.
35. Coletti, F., Macchietto, S., and Elvassore, N. Mathematical modeling of three-dimensional cell cultures in perfusion bioreactors. Ind Eng Chem Res **45,** 8158, 2006.
36. Martin, I., Wendt, D., and Heberer, M. The role of bioreactors in tissue engineering. Trends Biotechnol **22,** 80, 2004.
37. Klein-Nulend, J., *et al.* Sensitivity of osteocytes to biomechanical stress *in vitro*. FASEB J **9,** 441, 1995.
38. Piekarski, K., and Munro, M. Transport mechanism operating between blood supply and osteocytes in long bones. Nature **269,** 80, 1977.
39. Knothe Tate, M.L., and Knothe, U. An *ex vivo* model to study transport processes and fluid flow in loaded bone. J Biomech **33,** 247, 2000.
40. Klein-Nulend, J., Roelofsen, J., Semeins, C.M., Bronckers, A.L., and Burger, E.H. Mechanical stimulation of osteopontin mRNA expression and synthesis in bone cell cultures. J Cell Physiol **170,** 174, 1997.
41. Mullender, M., *et al.* Mechanotransduction of bone cells *in vitro*: mechanobiology of bone tissue. Med Biol Eng Comput **42,** 14, 2004.
42. Toma, C.D., Ashkar, S., Gray, M.L., Schaffer, J.L., and Gerstenfeld, L.C. Signal transduction of mechanical stimuli is dependent on microfilament integrity: identification of osteopontin as a mechanically induced gene in osteoblasts. J Bone Miner Res **12,** 1626, 1997.
43. Tong, L., Buchman, S.R., Ignelzi, M.A., Jr., Rhee, S., and Goldstein, S.A. Focal adhesion kinase expression during mandibular distraction osteogenesis: evidence for mechanotransduction. Plast Reconstr Surg **111,** 211; discussion 223, 2003.
44. Nauman, E.A., Satcher, R.L., Keaveny, T.M., Halloran, B.P., and Bikle, D.D. Osteoblasts respond to pulsatile fluid flow with shortterm increases in PGE(2) but no change in mineralization. J Appl Physiol **90,** 1849, 2001.
45. Claveau, D., *et al.* Microsomal prostaglandin E synthase-1 is a major terminal synthase that is selectively up-regulated during cyclooxygenase-2-dependent prostaglandin E2 production in the rat adjuvant-induced arthritis model. J Immunol **170,** 4738, 2003.

46. Waclawik, A., Blitek, A., and Ziecik, A.J. Oxytocin and tumor necrosis factor alpha stimulate expression of prostaglandin E2 synthase and secretion of prostaglandin E2 by luminal epithelial cells of the porcine endometrium during early pregnancy. Reproduction **140,** 613, 2010.
47. Salvado, M.D., Alfranca, A., Escolano, A., Haeggstrom, J.Z., and Redondo, J.M. COX-2 limits prostanoid production in activated HUVECs and is a source of PGH2 for transcellular metabolism to PGE2 by tumor cells. Arterioscler Thromb Vasc Biol **29,** 1131, 2009.
48. Murakami, M., *et al.* Regulation of prostaglandin E-2 biosynthesis by inducible membrane-associated prostaglandin E-2 synthase that acts in concert with cyclooxygenase-2. J Biol Chem **275,** 32783, 2000.

Address correspondence to:
Gordana Vunjak-Novakovic, PhD
Laboratory for Stem Cells and Tissue Engineering
Department of Biomedical Engineering
Columbia University
622 W168th St.
Vanderbilt Clinic 12-234
New York, NY 10032

E-mail: gv2131@columbia.edu

Received: December 12, 2011
Accepted: December 7, 2012
Online Publication Date: January 31, 2013